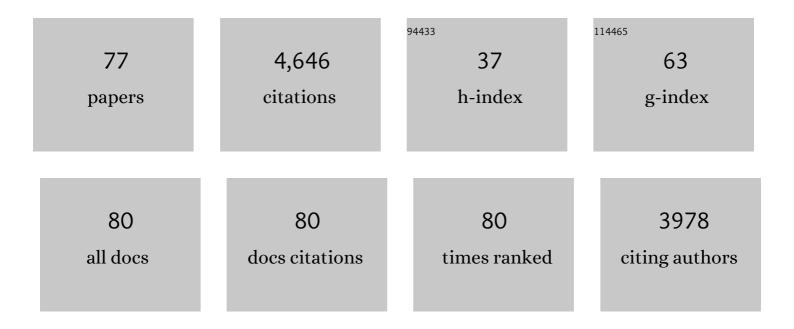
List of Publications by Year in descending order

Source: https://exaly.com/author-pdf/4899622/publications.pdf Version: 2024-02-01



#	Article	IF	CITATIONS
1	Surface and lightning sources of nitrogen oxides over the United States: Magnitudes, chemical evolution, and outflow. Journal of Geophysical Research, 2007, 112, .	3.3	279
2	Effect of petrochemical industrial emissions of reactive alkenes and NOxon tropospheric ozone formation in Houston, Texas. Journal of Geophysical Research, 2003, 108, .	3.3	263
3	Analysis of the atmospheric distribution, sources, and sinks of oxygenated volatile organic chemicals based on measurements over the Pacific during TRACE-P. Journal of Geophysical Research, 2004, 109, .	3.3	228
4	Boreal forest fire emissions in fresh Canadian smoke plumes: C ₁ -C ₁₀ volatile organic compounds (VOCs), CO ₂ , CO, NO _{2_{, NO, HCN and}}	4.9	209
5	CH ₃ CN. Atmospheric Chemistry and Physics, 2011, 11, 6445-6463. Ozone production rates as a function of NOxabundances and HOxproduction rates in the Nashville urban plume. Journal of Geophysical Research, 2002, 107, ACH 7-1.	3.3	207
6	OH and HO2concentrations, sources, and loss rates during the Southern Oxidants Study in Nashville, Tennessee, summer 1999. Journal of Geophysical Research, 2003, 108, .	3.3	174
7	The Deep Convective Clouds and Chemistry (DC3) Field Campaign. Bulletin of the American Meteorological Society, 2015, 96, 1281-1309.	3.3	165
8	Primary and secondary sources of formaldehyde in urban atmospheres: Houston Texas region. Atmospheric Chemistry and Physics, 2012, 12, 3273-3288.	4.9	153
9	Signatures of terminal alkene oxidation in airborne formaldehyde measurements during TexAQS 2000. Journal of Geophysical Research, 2003, 108, n/a-n/a.	3.3	126
10	Measured and modeled CO and NO y in DISCOVER-AQ: An evaluation of emissions and chemistry over the eastern US. Atmospheric Environment, 2014, 96, 78-87.	4.1	114
11	Evaluation of GOME satellite measurements of tropospheric NO2and HCHO using regional data from aircraft campaigns in the southeastern United States. Journal of Geophysical Research, 2004, 109, .	3.3	113
12	High levels of molecular chlorine in the Arctic atmosphere. Nature Geoscience, 2014, 7, 91-94.	12.9	105
13	Observing atmospheric formaldehyde (HCHO) from space: validation and intercomparison of six retrievals from four satellites (OMI, COME2A, COME2B, OMPS) with SEAC ⁴ RS aircraft observations over the southeast US. Atmospheric Chemistry and Physics, 2016, 16, 13477-13490.	4.9	99
14	Laboratory, ground-based, and airborne tunable diode laser systems: performance characteristics and applications in atmospheric studies. Applied Physics B: Lasers and Optics, 1998, 67, 317-330.	2.2	98
15	New insights into the column CH ₂ O/NO ₂ ratio as an indicator of nearâ€surface ozone sensitivity. Journal of Geophysical Research D: Atmospheres, 2017, 122, 8885-8907.	3.3	87
16	Summertime influence of Asian pollution in the free troposphere over North America. Journal of Geophysical Research, 2007, 112, .	3.3	86
17	Coupled evolution of BrOx-ClOx-HOx-NOxchemistry during bromine-catalyzed ozone depletion events in the arctic boundary layer. Journal of Geophysical Research, 2003, 108, .	3.3	82
18	The Korea–United States Air Quality (KORUS-AQ) field study. Elementa, 2021, 9, 1-27.	3.2	82

#	Article	IF	CITATIONS
19	Compact highly sensitive multi-species airborne mid-IR spectrometer. Applied Physics B: Lasers and Optics, 2015, 119, 119-131.	2.2	79
20	Ozone depletion events observed in the high latitude surface layer during the TOPSE aircraft program. Journal of Geophysical Research, 2003, 108, TOP 4-1.	3.3	75
21	First demonstration of a high performance difference frequency spectrometer on airborne platforms. Optics Express, 2007, 15, 13476.	3.4	74
22	Testing fast photochemical theory during TRACE-P based on measurements of OH, HO2, and CH2O. Journal of Geophysical Research, 2004, 109, .	3.3	71
23	Ultra-high-precision mid-IR spectrometer II: system description and spectroscopic performance. Applied Physics B: Lasers and Optics, 2006, 85, 207-218.	2.2	71
24	Observations of inorganic bromine (HOBr, BrO, and Br ₂) speciation at Barrow, Alaska, in spring 2009. Journal of Geophysical Research, 2012, 117, .	3.3	71
25	Nitrous acid (HONO) during polar spring in Barrow, Alaska: A net source of OH radicals?. Journal of Geophysical Research, 2011, 116, .	3.3	69
26	Airborne tunable diode laser measurements of formaldehyde during TRACE-P: Distributions and box model comparisons. Journal of Geophysical Research, 2003, 108, .	3.3	68
27	Revisiting the effectiveness of HCHO/NO2 ratios for inferring ozone sensitivity to its precursors using high resolution airborne remote sensing observations in a high ozone episode during the KORUS-AQ campaign. Atmospheric Environment, 2020, 224, 117341.	4.1	65
28	High-resolution inversion of OMI formaldehyde columns to quantify isoprene emission on ecosystem-relevant scales: application to the southeast US. Atmospheric Chemistry and Physics, 2018, 18, 5483-5497.	4.9	64
29	Tunable diode laser measurements of formaldehyde during the TOPSE 2000 study: Distributions, trends, and model comparisons. Journal of Geophysical Research, 2003, 108, .	3.3	62
30	Hydrogen peroxide, methyl hydroperoxide, and formaldehyde over North America and the North Atlantic. Journal of Geophysical Research, 2007, 112, .	3.3	58
31	Steady state free radical budgets and ozone photochemistry during TOPSE. Journal of Geophysical Research, 2003, 108, .	3.3	57
32	Design and performance of a tunable diode laser absorption spectrometer for airborne formaldehyde measurements. Journal of Geophysical Research, 2003, 108, .	3.3	54
33	On the effectiveness of nitrogen oxide reductions as a control over ammonium nitrate aerosol. Atmospheric Chemistry and Physics, 2016, 16, 2575-2596.	4.9	53
34	Large-scale ozone and aerosol distributions, air mass characteristics, and ozone fluxes over the western Pacific Ocean in late winter/early spring. Journal of Geophysical Research, 2003, 108, .	3.3	46
35	Detailed comparisons of airborne formaldehyde measurements with box models during the 2006 INTEX-B and MILAGRO campaigns: potential evidence for significant impacts of unmeasured and multi-generation volatile organic carbon compounds. Atmospheric Chemistry and Physics, 2011, 11, 11867-11894.	4.9	46
36	Peroxy radical behavior during the Transport and Chemical Evolution over the Pacific (TRACE-P) campaign as measured aboard the NASA P-3B aircraft. Journal of Geophysical Research, 2003, 108, .	3.3	44

#	Article	IF	CITATIONS
37	Revisiting global fossil fuel and biofuel emissions of ethane. Journal of Geophysical Research D: Atmospheres, 2017, 122, 2493-2512.	3.3	43
38	Comparisons of box model calculations and measurements of formaldehyde from the 1997 North Atlantic Regional Experiment. Journal of Geophysical Research, 2002, 107, ACH 3-1.	3.3	42
39	Vertical profiles of HDO/H2O in the troposphere. Journal of Geophysical Research, 2005, 110, .	3.3	40
40	Large vertical gradient of reactive nitrogen oxides in the boundary layer: Modeling analysis of DISCOVERâ€AQ 2011 observations. Journal of Geophysical Research D: Atmospheres, 2016, 121, 1922-1934.	3.3	38
41	Evaluation of simulated O3 production efficiency during the KORUS-AQ campaign: Implications for anthropogenic NOx emissions in Korea. Elementa, 2019, 7, .	3.2	38
42	Impact of the deep convection of isoprene and other reactive trace species on radicals and ozone in the upper troposphere. Atmospheric Chemistry and Physics, 2012, 12, 1135-1150.	4.9	33
43	Estimating Methane Emissions From Underground Coal and Natural Gas Production in Southwestern Pennsylvania. Geophysical Research Letters, 2019, 46, 4531-4540.	4.0	32
44	Observation-based modeling of ozone chemistry in the Seoul metropolitan area during the Korea-United States Air Quality Study (KORUS-AQ). Elementa, 2020, 8, .	3.2	32
45	An inversion of NO _{<i>x</i>} and non-methane volatile organic compound (NMVOC) emissions using satellite observations during the KORUS-AQ campaign and implications for surface ozone over East Asia. Atmospheric Chemistry and Physics. 2020. 20. 9837-9854.	4.9	30
46	Interactions of bromine, chlorine, and iodine photochemistry during ozone depletions in Barrow, Alaska. Atmospheric Chemistry and Physics, 2015, 15, 9651-9679.	4.9	29
47	Wet scavenging of soluble gases in DC3 deep convective storms using WRFâ€Chem simulations and aircraft observations. Journal of Geophysical Research D: Atmospheres, 2016, 121, 4233-4257.	3.3	29
48	Convective transport of formaldehyde to the upper troposphere and lower stratosphere and associated scavenging in thunderstorms over the central United States during the 2012 DC3 study. Journal of Geophysical Research D: Atmospheres, 2016, 121, 7430-7460.	3.3	28
49	Difference frequency generation spectrometer for simultaneous multispecies detection. Optics Express, 2010, 18, 27670.	3.4	27
50	Characterization of soluble bromide measurements and a case study of BrO observations during ARCTAS. Atmospheric Chemistry and Physics, 2012, 12, 1327-1338.	4.9	27
51	Convective transport and scavenging of peroxides by thunderstorms observed over the central U.S. during DC3. Journal of Geophysical Research D: Atmospheres, 2016, 121, 4272-4295.	3.3	24
52	Impacts of the Denver Cyclone on regional air quality and aerosol formation in the Colorado Front Range during FRAPPÉÂ2014. Atmospheric Chemistry and Physics, 2016, 16, 12039-12058.	4.9	24
53	The NO _{<i>x</i>} dependence of bromine chemistry in the Arctic atmospheric boundary layer. Atmospheric Chemistry and Physics, 2015, 15, 10799-10809.	4.9	23
54	Multispecies Assessment of Factors Influencing Regional CO ₂ and CH ₄ Enhancements During the Winter 2017 ACTâ€America Campaign. Journal of Geophysical Research D: Atmospheres, 2020, 125, e2019JD031339.	3.3	23

#	Article	IF	CITATIONS
55	Tunable diode laser studies of the reaction of Cl atoms with CH3CHO. International Journal of Chemical Kinetics, 1999, 31, 766-775.	1.6	22
56	Using Observations and Sourceâ€Specific Model Tracers to Characterize Pollutant Transport During FRAPPÉ and DISCOVERâ€AQ. Journal of Geophysical Research D: Atmospheres, 2017, 122, 10510-10538.	3.3	22
57	Formaldehyde column density measurements as a suitable pathway to estimate nearâ€surface ozone tendencies from space. Journal of Geophysical Research D: Atmospheres, 2016, 121, 13088-13112.	3.3	19
58	Modeling NH 4 NO 3 Over the San Joaquin Valley During the 2013 DISCOVERâ€AQ Campaign. Journal of Geophysical Research D: Atmospheres, 2018, 123, 4727-4745.	3.3	18
59	Forward Modeling and Optimization of Methane Emissions in the South Central United States Using Aircraft Transects Across Frontal Boundaries. Geophysical Research Letters, 2019, 46, 13564-13573.	4.0	18
60	The Atmospheric Carbon and Transport (ACT)-America Mission. Bulletin of the American Meteorological Society, 2021, 102, E1714-E1734.	3.3	17
61	Analysis of Oil and Gas Ethane and Methane Emissions in the Southcentral and Eastern United States Using Four Seasons of Continuous Aircraft Ethane Measurements. Journal of Geophysical Research D: Atmospheres, 2021, 126, e2020JD034194.	3.3	16
62	Effects of Scavenging, Entrainment, and Aqueous Chemistry on Peroxides and Formaldehyde in Deep Convective Outflow Over the Central and Southeast United States. Journal of Geophysical Research D: Atmospheres, 2018, 123, 7594-7614.	3.3	15
63	Atmospheric Carbon and Transport – America (ACTâ€America) Data Sets: Description, Management, and Delivery. Earth and Space Science, 2021, 8, e2020EA001634.	2.6	15
64	Photochemistry in the Arctic Free Troposphere: Ozone Budget and Its Dependence on Nitrogen Oxides and the Production Rate of Free Radicals. Journal of Atmospheric Chemistry, 2004, 47, 107-138.	3.2	14
65	Characterizing CO and NO _{<i>y</i>} Sources and Relative Ambient Ratios in the Baltimore Area Using Ambient Measurements and Source Attribution Modeling. Journal of Geophysical Research D: Atmospheres, 2018, 123, 3304-3320.	3.3	14
66	Sources and characteristics of summertime organic aerosol in the Colorado Front Range: perspective from measurements and WRF-Chem modeling. Atmospheric Chemistry and Physics, 2018, 18, 8293-8312.	4.9	13
67	Atmospheric Implications of Large C ₂ ₅ Alkane Emissions From the U.S. Oil and Gas Industry. Journal of Geophysical Research D: Atmospheres, 2019, 124, 1148-1169.	3.3	12
68	Spatial and temporal variability of trace gas columns derived from WRF/Chem regional model output: Planning for geostationary observations of atmospheric composition. Atmospheric Environment, 2015, 118, 28-44.	4.1	11
69	Estimator of Surface Ozone Using Formaldehyde and Carbon Monoxide Concentrations Over the Eastern United States in Summer. Journal of Geophysical Research D: Atmospheres, 2018, 123, 7642-7655.	3.3	11
70	Contrasting aerosol refractive index and hygroscopicity in the inflow and outflow of deep convective storms: Analysis of airborne data from DC3. Journal of Geophysical Research D: Atmospheres, 2017, 122, 4565-4577.	3.3	10
71	Impacts of physical parameterization on prediction of ethane concentrations for oil and gas emissions in WRF-Chem. Atmospheric Chemistry and Physics, 2018, 18, 16863-16883.	4.9	10
72	Photochemical evolution of the 2013 California Rim Fire: synergistic impacts of reactive hydrocarbons and enhanced oxidants. Atmospheric Chemistry and Physics, 2022, 22, 4253-4275.	4.9	9

#	Article	IF	CITATIONS
73	The Role of Snow in Controlling Halogen Chemistry and Boundary Layer Oxidation During Arctic Spring: A 1D Modeling Case Study. Journal of Geophysical Research D: Atmospheres, 2022, 127, .	3.3	6
74	Vertical Transport, Entrainment, and Scavenging Processes Affecting Trace Gases in a Modeled and Observed SEAC 4 RS Case Study. Journal of Geophysical Research D: Atmospheres, 2020, 125, e2019JD031957.	3.3	5
75	Can Column Formaldehyde Observations Inform Air Quality Monitoring Strategies for Ozone and Related Photochemical Oxidants?. Journal of Geophysical Research D: Atmospheres, 2022, 127, .	3.3	5
76	Autonomous airborne mid-infrared spectrometer for high-precision measurements of ethane during the NASA ACT-America studies. Atmospheric Measurement Techniques, 2020, 13, 6095-6112.	3.1	2
77	Tunable diode laser absorption spectroscopy for measuring atmospheric molecular species. , 0, , .		0